Stranglehold on the Spindle Assembly Checkpoint:

The Human Papillomavirus E2 Protein Provokes BUBR1-dependent Aneuploidy

Tan et al.

SUPPLEMENTARY DATA

SUPPLEMENTARY MATERIALS AND METHODS

Immunoprecipitation for Mass Spectrometry (MS) and MS data analyses

We performed 3 independent rounds of infections followed by MS including 2 replicates. Experiments #1 and #2 (replicates) were 2-step immunoprecipitations followed by classic LC-MS/MS, while experiment #3 was a single-step immunoprecipitation. In experiment #3, we employed SILAC (Stable Isotope Labeling by Amino-acids in Cell culture), a quantitative LC-MS/MS based approach which allowed us to verify and quantify and validate the interactions characterized in the first 2 MS. Each time, C33-A cells were infected with recombinant adenoviruses expressing 3xFlag-GFP-E2 and 3xFlag-GFP at a multiplicity of infection (m.o.i) of 20. This m.o.i gives levels of protein expression roughly one tenth of that found in HPV-18-infected cervical cells in vivo (physiological levels are approximately achieved by infection at m.o.i. 200).[1,2] After 24 hours, proteins were extracted (300mM NaCl, 0.5% NP-40, 50mM Tris-HCl [pH 8], 1mM EDTA, protease and phosphatase inhibitors) and subjected to immunoprecipitation.

For MS experiments #1 and #2, 20 mg of total proteins were immunoprecipitated in a two-step pull-down using first anti-Flag beads (A2220; Sigma-Aldrich) followed by elution, and second immunoprecipitation with GFP-Trap®_A beads (ChromoTek). Eluted protein complexes were separated by one-dimensional 4-12% NuPage Novex Bis-Tris Gel from Invitrogen (Supplementary Figures S1A and S1B), stained using the Colloidal Blue Staining Kit (Invitrogen) and digested with trypsin using published procedures.[3] The peptide samples were then subjected to nano LC and high resolution MS analysis. Samples were analyzed on an EASY-nanoLC (Proxeon) coupled to an Orbitrap or Orbitrap XL (Thermo Scientific). Survey full scan MS spectra (m/z 310–1400) were acquired with a resolution of r=60,000 at m/z 400, an AGC target of 1e6, and a maximum injection time of 500ms. The ten most intense peptide ions in each survey scan with an ion intensity >2000 counts and charge state ≥2 were isolated sequentially to a target value of 1e4, and fragmented in the linear ion trap by collisionally-induced dissociation using a normalized collision energy of 35%. A dynamic exclusion was applied using a maximum exclusion list of 500 with one repeat count and exclusion duration of 30 seconds. MS data of the first 2 experiments were analyzed using X!Tandem (version TORNADO (2008.02.01.4)). X!Tandem was set up to search against an in-house database that included the ncbi human database (ftp://ftp.ncbi.nih.gov/refseq/H_sapiens/H_sapiens/ARCHIVE/BUILD.37.1/protein) and HPV-18 databases assuming trypsin enzyme digestion. A fragment ion mass tolerance of 0.50 Da and a parent ion tolerance of

7.0 ppm were used. Iodoacetamide derivative of cysteine was specified as a fixed modification. Pyroglutamic acid from Glu of glutamic acid, pyroglutamic acid from Gln of glutamine, deamidation of asparagine, oxidation of methionine, and acetylation of the N terminus were specified as variable modifications. Scaffold (version Scaffold_2_05_02, Proteome Software, Inc., Portland, OR) was used to validate MS/MS-based peptide and protein identifications. For these 2 first MS, candidates detected only in the bait (Flag-GFP-E2) sample with 2 or more unique peptides and at least 2 spectral counts for both replicates were considered as interacting partners of E2 (GFP IP spectral counting must be 0). Common targets found in the 2 first independent MS experiments were analyzed using GeneGo (Supplementary Figures S1C and S1D) and further verified with the SILAC (Stable Isotope Labeling by Amino Acids in Cell Culture) experiment.

For this SILAC experiment (experiment #3), a SILAC approach was used before a single step immunoprecipitation with GFP-Trap®_A beads. Cells and samples were prepared as previously described.[4] Briefly, this technique allows metabolic incorporation of light or heavy amino-acids in all proteins of 2 distinct cell populations (e.g. GFP and GFP-E2). After immunoprecipitation, all proteins bounds to both control and bait are combined and loaded on gel in the same well before analysis by mass spectrometry (Supplementary Figure S1B, extreme right gel). Since both populations of proteins are labeled differentially, and are thus immediately identifiable, mass spectrometry allows direct quantitative analyses of abundance of one specific protein in the bait population compared to the control. SILAC data were searched using Mascot (version 2.2; Matrix Science, London, UK) against above databases. Cysteine carbamidomethylation was searched as a fixed modification, and N-acetylation and oxidized methionine were searched as variable modifications. Labeled arginine and lysine were specified as fixed or variable modifications, depending on the prior knowledge about the parent ion. SILAC peptide and protein quantification was performed with MaxQuant[5] using default settings. Maximum false discovery rates were set to 0.01 for both protein and peptide. For this SILAC experiments, proteins with a GFP-E2/GFP cut-off ratios $\geq$1.4 were considered as interacting partners.

SUPPLEMENTARY REFERENCES

1. Xue Y, Bellanger S, Zhang W, Lim D, Low J, Lunny D, Thierry F. HPV16 E2 is an immediate early marker of viral infection, preceding E7 expression in precursor structures of cervical carcinoma. Cancer Res 2010; 70:5316-25.
2. Bellanger S, Tan CL, Xue YZ, Teissier S, Thierry F. Tumor suppressor or oncogene? A critical role of the viral E2 protein in cervical cancer progression. Am J Cancer Res 2011; 1:373-89.
3. Shevchenko A, Tomas H, Havlis J, Olsen JV, Mann M. In-gel digestion for mass spectrometric characterization of proteins and proteomes. Nat Protoc 2006; 1:2856-60.
4. Gunaratne J, Goh MX, Swa HL, Lee FY, Sanford E, Wong LM, Hogue KA, Blackstock WP, Okumura K. Protein interactions of phosphatase and tensin homologue (PTEN) and its cancer-associated G20E mutant compared by using stable isotope labeling by amino acids in cell culture-based parallel affinity purification. J Biol Chem 2011; 286:18093-103.
5. Cox J, Mann M. MaxQuant enables high peptide identification rates, individualized p.p.b.-range mass accuracies and proteome-wide protein quantification. Nat Biotechnol 2008; 26:1367-72.

SUPPLEMENTARY TABLE S1

Symbol	Gene name and pathway	gi number	Spectral counting				SILAC	
			MS/MS #1		MS/MS #2			
			GFP-E2	GFP	GFP-E2	GFP	Ratio GFP-E2 / GFP	Ratio count
Spindle Assembly Checkpoint								
Cdc20	cell division cycle 20	gi|118402582	ND	ND	2	0	1.42	12
MAD2	mitotic spindle assembly checkpoint protein MAD2A	gi|4505067	2	0	ND	ND	3.3	4
BUBR1	BUB1 budding uninhibited by benzimidazoles 1 homolog beta	gi|59814247	8	0	10	0	1.78	15
Kinetochores and SAC regulation								
BRCA2	breast cancer 2, early onset	gi|119395734	4	0	6	0	ND	ND
NUP153	nucleoporin 153kDa	gi|24430146	22	0	35	0	11.19	54
CRM1	exportin 1	gi|4507943	8	0	19	0	1.41	34
DYNC1H1	cytoplasmic dynein 1, heavy chain 1	gi|33350932	22	0	27	0	ND	ND
SMC1A	structural maintenance of chromosomes 1A	gi|30581135	4	0	13	0	ND	ND
SMC3	structural maintenance of chromosomes 3	gi|4885399	4	0	11	0	1.43	3
DCTN1	dynactin 1, isoform 2	gi|13259508	10	0	5	0	ND	ND
Mitotic Spindle								
TPX2	targeting protein for Xklp2	gi|20127519	4	0	9	0	1.61	28
TUBA1A	tubulin alpha-1A chain isoform 1	gi|17986283	250	0	133	0	2.47	103
TUBA1C	tubulin alpha-1C chain	gi|14389309	250	0	151	0	2.47	18
TUBB6	tubulin beta-6 chain	gi|14210536	92	0	74	0	3.52	10
TUBB4	tubulin beta-4 chain	gi|21361322	264	0	128	0	2.72	8
TUBB3	tubulin beta-3 chain isoform 1	gi|50592996	214	0	125	0	2.91	16
TUBB2B	tubulin beta-2B chain	gi|29788768	278	0	138	0	ND	ND
TUBB4B	tubulin beta-4B chain	gi|5174735	314	0	163	0	2.5	10
TUBG1	tubulin gamma-1 chain	gi|12653673	4	0	4	0	1.59	4
KIF22	kinesin-like protein KIF22 isoform 1	gi|6453818	4	0	11	0	2.9	7
MAP1B	microtubule-associated protein 1B	gi|153945728	28	0	20	0	ND	ND

Supplementary Table S1. List of E2 interactors involved in the SAC, kinetochore and SAC regulation, and mitotic Spindle. C33-A cells were infected with recombinant adenoviruses. Three independent sets of infections and immunoprecipitations were performed and bound proteins were analyzed by mass spectrometry (2 LC-MS/MS [replicates] and 1 SILAC-based MS). GFP-E2 was used as bait, GFP was used as control as indicated. The table shows the spectral counting found by MS corresponding to each protein interacting with HPV-18 E2 in the 2 first MS. SILAC ratio: normalized ratio between the heavy and light SILAC states. Ratio count: number of SILAC measurements used to calculate the peptide ratio. ND: Not Detected.

SUPPLEMENTARY FIGURE S1

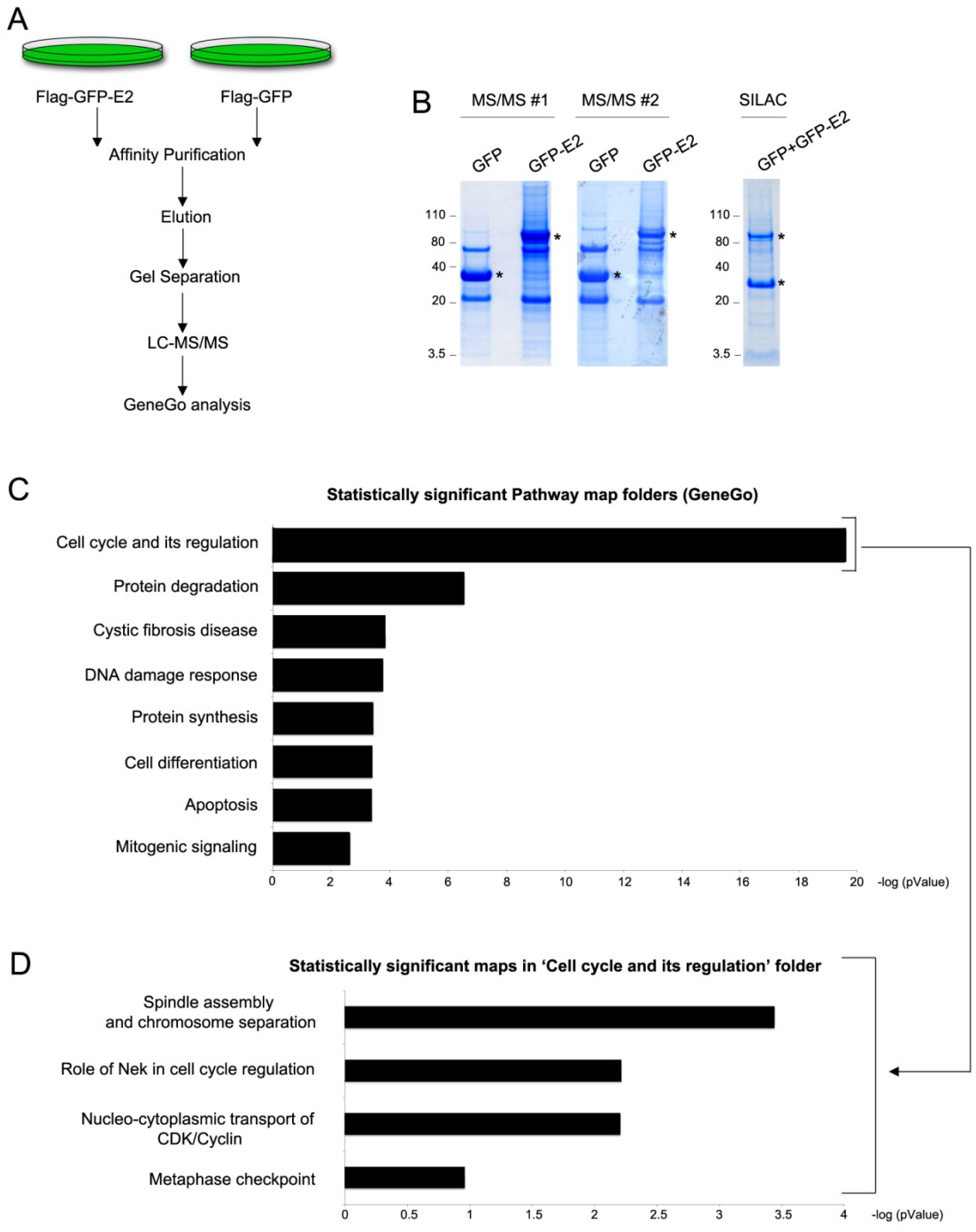

Supplementary Figure S1. Mass Spectrometry (MS) analyses of the E2 interactome. (**A**) Workflow for identification of E2 interactants by affinity purification followed by LC-MS/MS analysis. (**B**) Coomassie blue staining of the immunoprecipitates before mass spectrometry analysis. Asterisks show GFP and GFP-E2 bands. (**C**) A total of 406 proteins were found to interact with E2 in the 2 first MS experiments and were sorted into clusters by GeneGo analysis software. Most significant "Pathway map folders" are shown. (**D**). Most significant maps in the "Cell cycle and its regulation" folder (from above) are shown.

SUPPLEMENTARY FIGURE S2

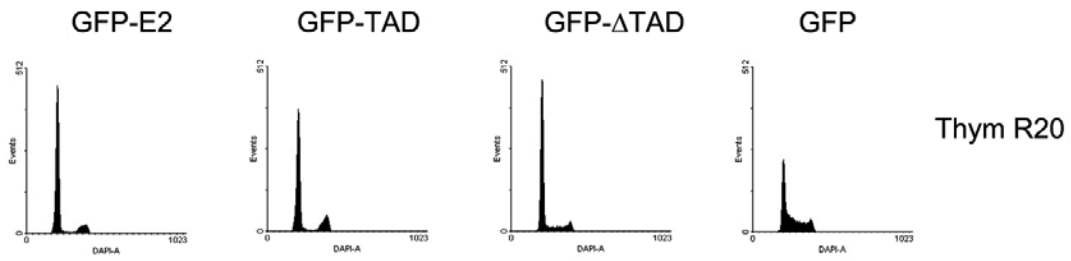

Supplementary Figure S2: Control experiment showing that cells from Figure 3A were blocked in mitosis by nocodazole and not by E2. In Figure 3A, cells were first blocked at the G1/S transition by thymidine, released for 6 hours (they were in G2 at this time-point) and simultaneously treated by nocodazole and infected with recombinant adenoviruses. Since expression of recombinant proteins from adenoviruses only starts from 8 hours onwards after infection, whereas the cells enter in mitosis between 4 and 6 hours after beginning of G2, in theory cells should be blocked in mitosis by nocodazole before they start expressing E2. Therefore, infection by AdGFP-E2 should have no effect on mitosis 4-6 hours after infection, and the cells should be able to exit mitosis normally if not treated by nocodazole. However, we absolutely needed to verify this, especially because a very low level of E2 is sufficient to arrest cells in mitosis. For this, we performed a control experiment in parallel where the nocodazole was omitted (and replaced by DMSO) following thymidine release. If the level of E2 in mitosis was sufficient to induce a mitotic arrest 6 hours after thymidine release, at least a percentage of cells would appear blocked in mitosis 20h after thymidine release in the absence of nocodazole (as we have shown in Figure 1B where cells were infected at the beginning of the thymidine treatment, therefore around 36 hours before mitosis). Here, 20 hours after thymidine release, GFP-E2- and GFP-TAD-expressing cells showed no arrest in mitosis in the absence of nocodazole treatment, demonstrating that indeed, the mitotic block observed in the nocodazole treated samples was due to SAC avtivation by nocodazole and not by E2. A western-blot showing the relative quantities of the different proteins at TR20 is shown in Fig. S3A

SUPPLEMENTARY FIGURE S3

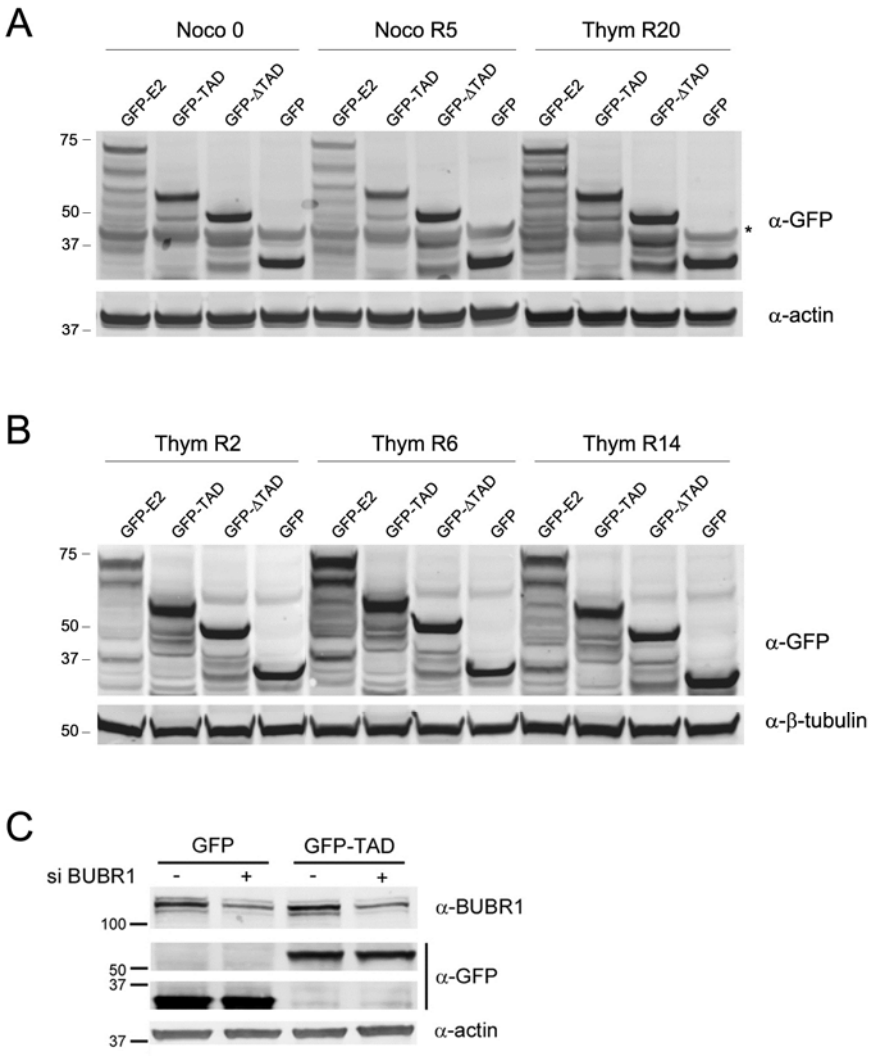

Supplementary Figure S3. Western-Blot showing the relative quantities of proteins for Figures 3A (and S2), 3B and 5. (**A**) Western-blot showing the relative quantities of the indicated proteins at the different time-points for Figures 3A and S2. The asterisk corresponds to the actin band which was probed first. (**B**) Western-blot showing the relative quantities of the indicated proteins at the different time-points from Figure 3B. (**C**) Western-blot showing decrease in BUBR1 levels after silencing of BUBR1 in both GFP- and GFP-TAD-expressing cells (cells from Figure 5).

SUPPLEMENTARY FIGURE S4

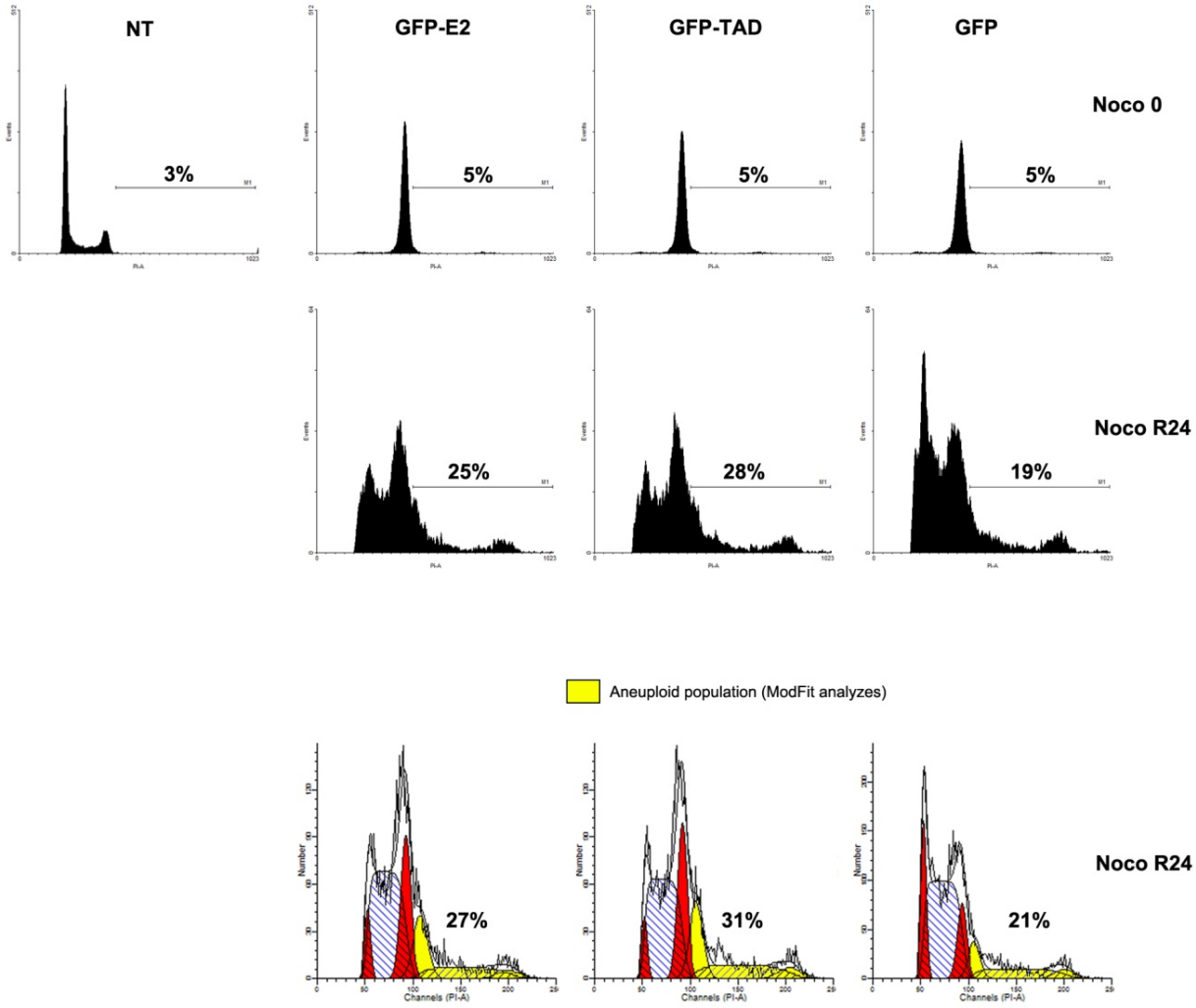

Supplementary Figure S4. The aneuploid population is enhanced by E2 and TAD expression compared to GFP 24 hours after release from nocodazole. Cell cycle analyses of HeLa cells expressing GFP-E2, GFP-TAD or GFP. Cells were synchronized in pro-metaphase by successive thymidine/nocodazole treatments as in Figure 3A. NT = asynchronous and not infected cells. Infection was performed at Thym R6 together with nocodazole treatment. After mitotic shake-off (14 hours after infection and nocodazole treatment, Noco 0), cells were released for 24 hours in fresh medium (Noco R24). The aneuploid population was calculated using WinMDI (black graphs) and ModFit (colored graphs)

SUPPLEMENTARY FIGURE S5

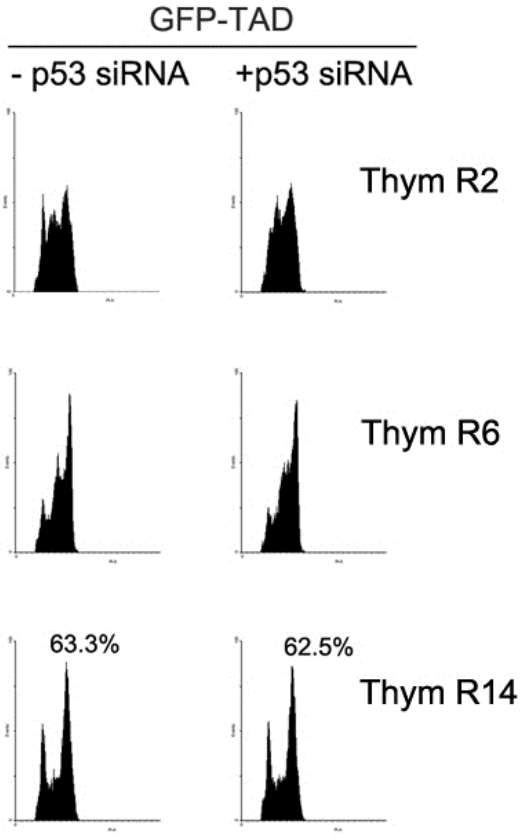

Supplementary Figure S5. Silencing p53 does not enhance TAD-induced arrest in mitosis. Cell cycle analyses of HeLa cells expressing GFP-TAD transfected with either a control siRNA or a siRNA against p53, synchronized in S phase (Thym R2), and released for 4 hours (Thym R6) or 12 hours (Thym R14).

LEGENDS TO SUPPLEMENTARY MOVIES

Supplementary Movie S1. Time-lapse experiment performed with synchronized HeLa cells expressing GFP-TAD and transfected with a control siRNA (siCtrl). Phase contrast images are shown.

Supplementary Movie S2. Time-lapse experiment performed with synchronized HeLa cells expressing GFP and transfected with a control siRNA (siCtrl). Phase contrast images are shown.

Supplementary Movie S3. Time-lapse experiment (high magnification + DNA staining) performed with synchronized HeLa cells expressing GFP-TAD and transfected with a control siRNA (siCtrl). Phase contrast images are shown as well as fluorescence images obtained after staining DNA with Hoechst.

Supplementary Movie S4. Time-lapse experiment performed with synchronized HeLa cells expressing GFP-TAD and transfected with a siRNA against BUBR1 (siBUBR1). Phase contrast images are shown.

Supplementary Movie S5. Time-lapse experiments performed with synchronized HeLa cells expressing GFP and transfected with a siRNA against BUBR1 (siBUBR1). Phase contrast images are shown.

Supplementary Movie S6. Time-lapse experiment (high magnification + DNA staining) performed with synchronized HeLa cells expressing GFP-TAD and transfected with a siRNA against BUBR1 (siBUBR1). Phase contrast images are shown as well as fluorescence images obtained after staining DNA with Hoechst.